Physics Letters B 735 (2014) 305–310

Contents lists available at ScienceDirect

Physics Letters B

www.elsevier.com/locate/physletb

How (non-)linear is the hydrodynamics of heavy ion collisions?

Stefan Floerchinger [a], Urs Achim Wiedemann [a,*], Andrea Beraudo [a,b], Luca Del Zanna [c,d,e], Gabriele Inghirami [c,d], Valentina Rolando [f,g]

[a] Physics Department, Theory Unit, CERN, CH-1211 Genève 23, Switzerland
[b] Dep. de Fisica de Particulas, U. de Santiago de Compostela, E-15782 Santiago de Compostela, Galicia, Spain
[c] Dipartimento di Fisica e Astronomia, Università di Firenze, Via G. Sansone 1, I-50019 Sesto F.no (Firenze), Italy
[d] INFN - Sezione di Firenze, Via G. Sansone 1, I-50019 Sesto F.no (Firenze), Italy
[e] INAF - Osservatorio Astrofisico di Arcetri, L.go E. Fermi 5, I-50125 Firenze, Italy
[f] INFN - Sezione di Ferrara, Via Saragat 1, I-44100 Ferrara, Italy
[g] Dipartimento di Fisica e Scienze della Terra, Università di Ferrara, Via Saragat 1, I-44100 Ferrara, Italy

ARTICLE INFO

Article history:
Received 26 January 2014
Received in revised form 4 June 2014
Accepted 17 June 2014
Available online 20 June 2014
Editor: J.-P. Blaizot

ABSTRACT

We provide evidence from full numerical solutions that the hydrodynamical evolution of initial density fluctuations in heavy ion collisions can be understood order-by-order in a perturbative series in deviations from a smooth and azimuthally symmetric background solution. To leading linear order, modes with different azimuthal wave numbers do not mix. When quadratic and higher order corrections are numerically sizable, they can be understood as overtones with corresponding wave numbers in a perturbative series. Several findings reported in the recent literature result naturally from the general perturbative series formulated here.

In recent years, fluid dynamic simulations of relativistic heavy ion collisions have provided strong evidence for a picture according to which the momentum distributions of soft hadrons result from a fluid dynamic evolution of initial density fluctuations, see Refs. [1–4] for recent reviews. The research focuses now on understanding in detail the mapping from fluctuations in the initial state to experimentally accessible observables in the final state [5–16]. While hydrodynamic evolution always shows non-linearities of some size, we ask here whether the hydrodynamics of heavy ion collisions is sufficiently weakly non-linear to be described by a perturbative series. We shall demonstrate that the fluid dynamic response to initial perturbations obeys a general ordering principle in that it can be organized in terms of a perturbative expansion in powers of the amplitudes of initial fluctuations around a background, see Eq. (2) below. This perturbative series will be shown to apply also in cases where non-linearities are sizable or dominant. This is of interest since a mapping in which non-linearities are organized as corrections to a linear response provides a particularly simple and thus particular powerful tool for relating experimental observables to the initial conditions of heavy ion collisions and to those properties of matter that govern their fluid dynamic evolution [17].

We consider initial conditions of heavy ion collisions, specified in terms of fluctuating fluid dynamic fields h_i on a hyper surface at fixed initial time τ_0. Here, the index i runs over all independent fields,

$$h_i(\tau, r, \varphi, \eta) = \big(w, u^r, u^\phi, u^\eta, \pi_{\rm bulk}, \pi^{\eta\eta}, \ldots\big), \tag{1}$$

including e.g. the enthalpy density $h_1 = w$, three independent fluid velocity components, the bulk viscous tensor, the independent components of the shear viscous tensor, etc. In the following we assume Bjorken boost invariance and drop the rapidity-argument η in the hydrodynamical fields. Following Refs. [17,18], we express h_i in terms of a background component h_i^{BG} and an appropriately normalized perturbation $\tilde{h}_i$. The background is taken to be a solution of the non-linear hydrodynamic equations initialized at τ_0 with an azimuthally symmetric average over many events. It is evolved with the fluid dynamic solver ECHO-QGP [19]. For any sample of events, this background needs to be determined only once. We ask to what extent the time evolution of the $\tilde{h}_i$, obtained from the full numerical ECHO-QGP solutions without any linearized approximation, can be understood in terms of a perturbative series on top of the background fields,

$$\tilde{h}_i(\tau, r, \varphi) = \int_{r',\varphi'} \mathscr{G}_{ij}\big(\tau, \tau_0, r, r', \varphi - \varphi'\big)\tilde{h}_j\big(\tau_0, r', \varphi'\big)$$

* Corresponding author.

http://dx.doi.org/10.1016/j.physletb.2014.06.049

$$+\frac{1}{2}\int_{r',r'',\varphi',\varphi''} \mathscr{H}_{ijk}(\tau,\tau_0,r,r',r'',\varphi-\varphi',\varphi-\varphi'') \times \tilde{h}_j(\tau_0,r',\varphi')\tilde{h}_k(\tau_0,r'',\varphi'')+\mathcal{O}(\tilde{h}^3), \quad (2)$$

where $\int_r = \int_0^\infty dr\, r$, $\int_\varphi = \int_0^{2\pi} d\varphi$ etc. The kernels $\mathscr{G}_{ij}$, $\mathscr{H}_{ijk}$ (and corresponding terms for higher orders in $\tilde{h}_i$) depend on the time-evolved background h_i^{BG} only. Due to the azimuthal rotation symmetry of the background, $\mathscr{G}_{ij}$ depends on the angles φ and φ' only via the difference $\varphi-\varphi'$ and similarly for $\mathscr{H}_{ijk}$. The question we raise in the title can now be made more precise: We ask whether the expansion (2) is possible for a suitably chosen background,[1] in which range it is dominated by the first linear term, and whether non-linearities even if large can be understood perturbatively on the basis of (2).

For the initial conditions, we make assumptions that are widely spread in the phenomenological literature. The initial transverse velocity components vanish, the longitudinal velocity is Bjorken boost invariant, the shear stress tensor is initialized by its Navier–Stokes value, and the bulk viscous pressure is neglected. Initial fluctuations reside then only in the initial enthalpy density $w(\tau,\vec{r})$, that we parametrize in terms of an azimuthally averaged background $w_{BG}(\tau,r)$ and the weights $\tilde{w}_l^{(m)}$ of the azimuthal (m) and radial (l) wave numbers of a discrete orthonormal Bessel–Fourier decomposition [17]

$$w(\tau_0,r,\varphi) = w_{BG}(\tau_0,r)\left(1+\sum_{m=-\infty}^{\infty}\tilde{w}^{(m)}(\tau_0,r)\,e^{im\varphi}\right),$$
$$\tilde{w}^{(m)}(\tau_0,r) = \sum_{l=1}^{\infty}\tilde{w}_l^{(m)}\,J_m\big(k_l^{(m)}r\big). \quad (3)$$

Here $k_l^{(m)} = z_l^{(m)}/R$, where $z_l^{(m)}$ is the l-th zero of the modified Bessel function J_m and $R=8$ fm throughout this work. Since $\tilde{w}(\tau,r,\varphi)$ is real, we have $\tilde{w}^{(m)}(\tau,r) = \tilde{w}^{(-m)*}(\tau,r)$. In the following, we take the weights with $m\geq 0$ as the independent ones and write

$$\tilde{w}_l^{(m)} = \big|\tilde{w}_l^{(m)}\big|e^{-im\psi_l^{(m)}}. \quad (4)$$

The corresponding modes with $m<0$ are then not independent and are defined by the condition $|\tilde{w}_l^{(m)}| = |\tilde{w}_l^{(-m)}|$ with azimuthal angle $\psi_l^{(-m)} = \psi_l^{(m)} \pm \pi$.

We next discuss the physically relevant range of $|\tilde{w}_l^{(m)}|$. For central heavy ion collisions, the event averaged weights $\langle|\tilde{w}_l^{(m)}|\rangle \simeq \mathcal{O}(0.1)$ and the tails of event distributions satisfy $|\tilde{w}_l^{(m)}| \lesssim 0.5$, see e.g. Fig. 13 of Ref. [18]. In peripheral collisions, event distributions shift to larger $|\tilde{w}_l^{(m)}|$ with increasing impact parameter b, since the expansion (3) is around an azimuthally symmetric background. Also in these non-central collisions, $\langle|\tilde{w}_l^{(m)}|\rangle$ is much smaller than unity (e.g. $\langle|\tilde{w}_l^{(m)}|\rangle \simeq 0.5$ at $b=6$ fm for the model in Ref. [18]). For an intuitive understanding of these values, one may consider the case for which one single fluctuating basis mode, say the mode with the weight $\tilde{w}_1^{(2)}$, is embedded on top of $w_{BG}(\tau_0,r)$

$$w(\tau_0,\vec{r}) = w_{BG}(\tau_0,r)\big[1+2\big|\tilde{w}_1^{(2)}\big|\,J_2\big(k_1^{(2)}r\big)\cos\big(2\big(\varphi-\psi_1^{(2)}\big)\big)\big]. \quad (5)$$

For one single mode, we can set without loss of generality $\psi_1^{(2)}=0$. The Bessel function J_2 takes a maximal value $\max[J_2(r)] = 0.4865$, and the enthalpy density (5) is therefore positive definite at all transverse positions only for $|\tilde{w}_1^{(2)}| < 1/(2\max[J_2(r)]) = 1.028$. Larger values for $|\tilde{w}_1^{(2)}|$ can arise only if the presence of additional modes $|\tilde{w}_l^{(m)}|$ ensures that the negative contribution from $|\tilde{w}_1^{(2)}|$ to $w(\tau_0,\vec{r})$ is canceled everywhere. The larger the cancellation needed, the smaller the probability that it arises in an event sample. This may provide an intuitive understanding for why even the tails of event distributions of peripheral collisions are confined to values $|\tilde{w}_1^{(2)}|$ smaller than 1.5, and why the most likely initial conditions show values that are $O(0.5)$ or smaller. Numerically similar constraints are obtained for other basis modes.

In Fig. 1, we test the fluid dynamic response to a single fluctuating basis mode (5) for the entire physically relevant parameter range $|\tilde{w}_l^{(m)}| < 1.5$. Assuming for simplicity a Bjorken-boost invariant longitudinal dependence, we evolve these initial conditions with the $2+1$ dimensional version of the hydrodynamical code ECHO-QGP [19] with a value $\eta/s = 1/4\pi$ for the ratio of shear viscosity to entropy density.[2] Following Ref. [20], we use the equation of state s95p-PCE which combines lattice QCD results at high temperatures with a hadron resonance gas at low temperatures. The background w_{BG} used throughout this paper is initialized at $\tau_0 = 0.6$ fm/c with an azimuthally symmetric average of Glauber model initial conditions for Pb+Pb collisions at the LHC, described in Ref. [18]. The time evolution of w_{BG} determined from ECHO-QGP is shown in Fig. 1. The time-evolved fluctuation $\tilde{w}^{(2)}(\tau,r)$ is determined from the full hydrodynamic evolution via Fourier analysis.[3] The main observation from Fig. 1 is that the fluid dynamic response to (5) scales approximately linearly with the initial amplitude $\tilde{w}_1^{(2)}$ of the perturbation. This scaling, expected from the linear term in Eq. (2), is very good for values $\tilde{w}_1^{(2)} < 0.6$. We observe this linear dependence with similar accuracy also for other basic modes (data not shown). More sizable deviations from linear scaling are observed for $\tilde{w}_1^{(2)} > 0.6$, see Fig. 1.

The main message of this work is that even for the largest physically relevant amplitudes $\tilde{w}_l^{(m)}$, where non-linear contributions can dominate the hydrodynamic response, the observed non-linearities can be understood in terms of the perturbative ansatz (2). To explain this point, we note first that the dominant non-linearity in the hydrodynamic response to a fluctuation with weights $w_1^{(2)}$ is in modes $m\neq 2$. Consider the Fourier series $\tilde{h}_i(\tau,r,\varphi) = \frac{1}{2\pi}\sum_{m=-\infty}^{\infty} e^{im\varphi}\,\tilde{h}_i^{(m)}(\tau,r)$, where $\tilde{h}_i^{(m)}(\tau,r)$ are in general complex expansion coefficients, but $\tilde{h}_i^{(m)}(\tau,r) = \tilde{h}_i^{(-m)*}(\tau,r)$ since $\tilde{h}(\tau,r,\varphi)\in\mathbb{R}$. Since the kernels in (2) depend only on the background field, they are invariant under azimuthal rotation and their Fourier expansions read

$$\mathscr{G}_{ij}\big(\tau,\tau_0,r,r',\Delta\varphi\big) = \frac{1}{2\pi}\sum_{m=-\infty}^{\infty} e^{im\Delta\varphi}\mathscr{G}_{ij}^{(m)}\big(\tau,\tau_0,r,r'\big),$$

[1] Hydrodynamic evolution is governed by non-linear partial differential equations and it may be chaotic or it may contain terms that are non-analytic in the initial fluid fields $\tilde{h}_j$. Hence, the validity of the expansion (2) is not guaranteed. Also, it will depend on the choice of the background h^{BG} and on the strength of the perturbations $\tilde{h}$.

[2] For these $2+1$ dimensional simulations in Bjorken coordinates, we adopt a uniform grid in x and y with a spatial resolution of 0.2 fm, whereas the time-step is set to 10^{-3} fm/c, with a Courant number of 0.2 to ensure stability. Spatial reconstruction is achieved by employing the MPE5 scheme, the most accurate one available in ECHO-QGP (fifth order for smooth flows). For further technical details, see Ref. [19].

[3] Fluctuations at time τ_0 are cut-off in the region of very low background density, see e.g. $\tilde{w}^{(2)}(\tau_0,r)$ in Fig. 1. Also, for the extreme weights $\tilde{w}_1^{(2)} = 1.2$ and 1.4, the distribution (5) is cut off in the regions in which it would turn negative. For values $|\tilde{w}_1^{(2)}| < 1/(2\max[J_2(r)]) = 1.028$, the single mode can be propagated without such an ad hoc modification. We have checked that these cuts do not affect our conclusions.

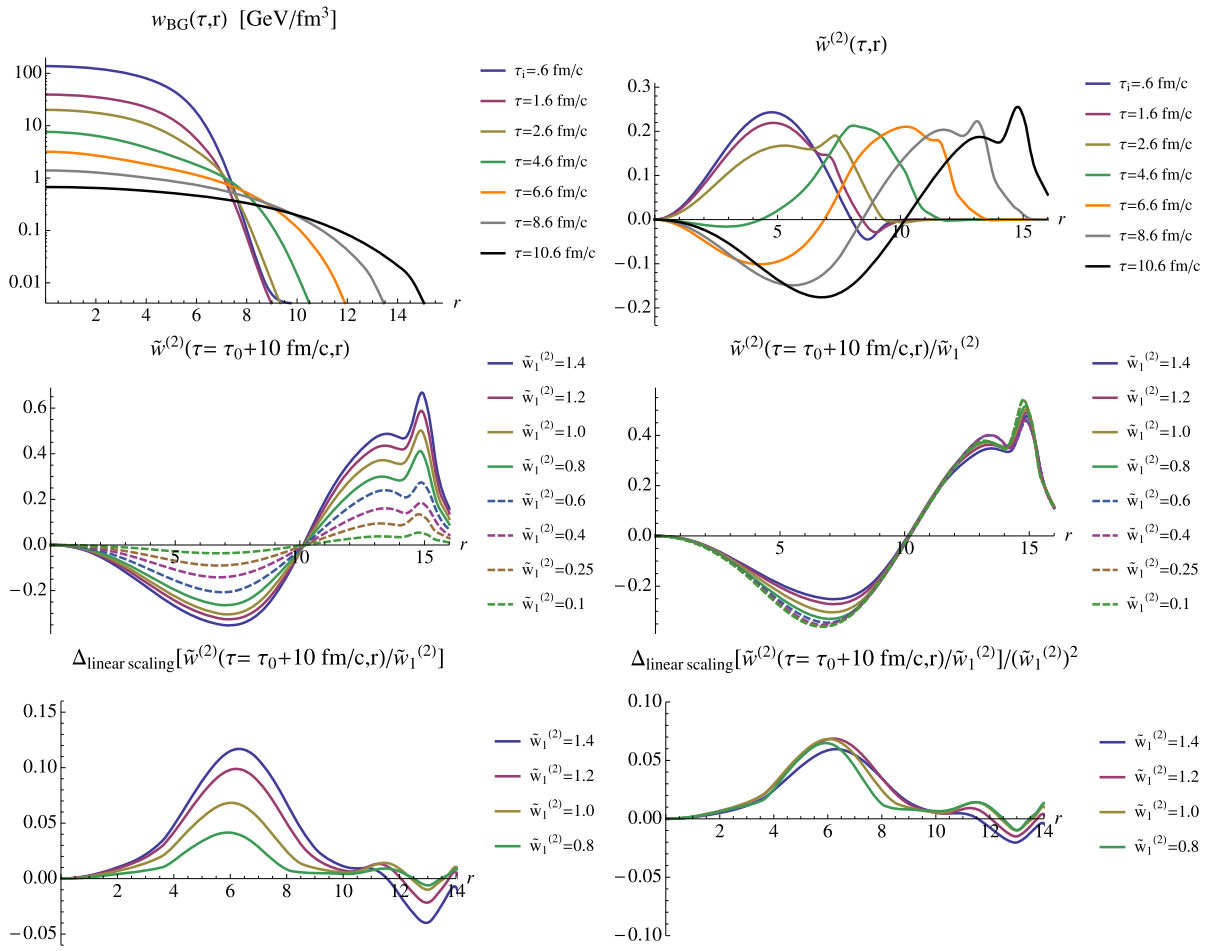

Fig. 1. The hydrodynamic evolution of the initial condition (5), obtained with ECHO-QGP. Upper row: The time dependence of the enthalpy density is shown separately for the background $w_{BG}(\tau,r)$ and for the perturbation $\tilde{w}^{(2)}(\tau,r)$ initialized with $\tilde{w}_1^{(2)}=0.5$. Middle row: The dependence of the perturbations $\tilde{w}^{(2)}$ on the initial weight for $\tau=\tau_0+10$ fm/c (left) and scaled by the initial weights, $\tilde{w}^{(2)}(\tau,r)/\tilde{w}_1^{(2)}$ (right). This scaling shows to what extent the fluid dynamic response to perturbations is approximately linear. Lower row: The deviation from linear scaling $\Delta_{\text{linear scaling}}=\tilde{w}^{(2)}(\tau,r)/\tilde{w}_1^{(2)}-\tilde{w}^{(2)}(\tau,r)/\tilde{w}_1^{(2)}|_{\tilde{w}_1^{(2)}=0.1}$. This quantity would vanish for perfect linear scaling and it scales with $O((\tilde{w}_1^{(2)})^2)$ if it is dominanted by the third order correction in (2). This scaling shows that non-linearities can be understood perturbatively in terms of Eq. (7).

$$\mathscr{H}_{ijk}(\tau,\tau_0,r,r',r'',\Delta\varphi',\Delta\varphi'') = \frac{1}{(2\pi)^2}\sum_{m',m''=-\infty}^{\infty} e^{i(m'\Delta\varphi'+m''\Delta\varphi'')}\,\mathscr{H}_{ijk}^{(m',m'')}(\tau,\tau_0,r,r',r''), \tag{6}$$

and so on. From $\mathscr{G}_{ij}(\tau,\tau_0,r,r',\Delta\varphi)\in\mathbb{R}$ one obtains $\mathscr{G}_{ij}^{(m)}=\mathscr{G}_{ij}^{(-m)*}$ and similarly $\mathscr{H}_{ijk}^{(m',m'')}=\mathscr{H}_{ijk}^{(-m',-m'')*}$. One obtains then from Eq. (2)

$$\begin{aligned}\tilde{h}_i^{(m)}(\tau,r) = {}& \int_{r'}\mathscr{G}_{ij}^{(m)}(\tau,\tau_0,r,r')\tilde{h}_j^{(m)}(\tau_0,r') \\ & + \frac{1}{2}\int_{r',r''}\frac{1}{2\pi}\sum_{m',m''}\delta_{m,m'+m''}\mathscr{H}_{ijk}^{(m',m'')}(\tau,\tau_0,r,r',r'') \\ & \times\tilde{h}_j^{(m')}(\tau_0,r')\tilde{h}_k^{(m'')}(\tau_0,r'')+\dots\end{aligned} \tag{7}$$

For the case that initial conditions contain only fluctuations of enthalpy density, we have $\tilde{h}_j^{(m)}(\tau_0,r)=\delta_{j1}\,\tilde{w}^{(m)}(\tau_0,r)$. Using the orthonormal expansion (3) for $\tilde{w}^{(m)}(\tau_0,r)$, one can write Eq. (7) as

$$\begin{aligned}\tilde{h}_i^{(m)}(\tau,r) = {}& \sum_{l'}\mathscr{G}_{i1;l'}^{(m)}(\tau,\tau_0,r)\tilde{w}_{l'}^{(m)} \\ & + \frac{1}{4\pi}\sum_{m',m'',l',l''}\delta_{m,m'+m''}\mathscr{H}_{i11;l'l''}^{(m',m'')}(\tau,\tau_0,r) \\ & \times\tilde{w}_{l'}^{(m')}\tilde{w}_{l''}^{(m'')}+\dots\end{aligned} \tag{8}$$

with

$$\mathscr{G}_{i1;l'}^{(m)}(\tau,\tau_0,r)=\int_{r'}\mathscr{G}_{i1}^{(m)}(\tau,\tau_0,r,r')\;J_m(k_{l'}^{(m)}r'), \tag{9}$$

and similarly for $\mathscr{H}_{i11;l'l''}$.

To explain how results in the recent literature are related to Eq. (8), we recall that the initial amplitudes $\tilde{w}_l^{(m)}$ are related linearly to the n-th radial moments that define the eccentricities $\epsilon_{m,n}$ [18]. A linear relationship between eccentricities and flow observable would thus correspond to a truncation of (8) at linear order. There is evidence that this is a good approximation for elliptic and triangular flow, $m=2,3$, see e.g. Ref. [12]. Also, it has been found that corrections quadratic in eccentricities can give sizable contributions to quadrangular and pentagonal flow coefficients when they involve at least one power of $\epsilon_{2,n}$ (or $\tilde{w}_l^{(2)}$ in

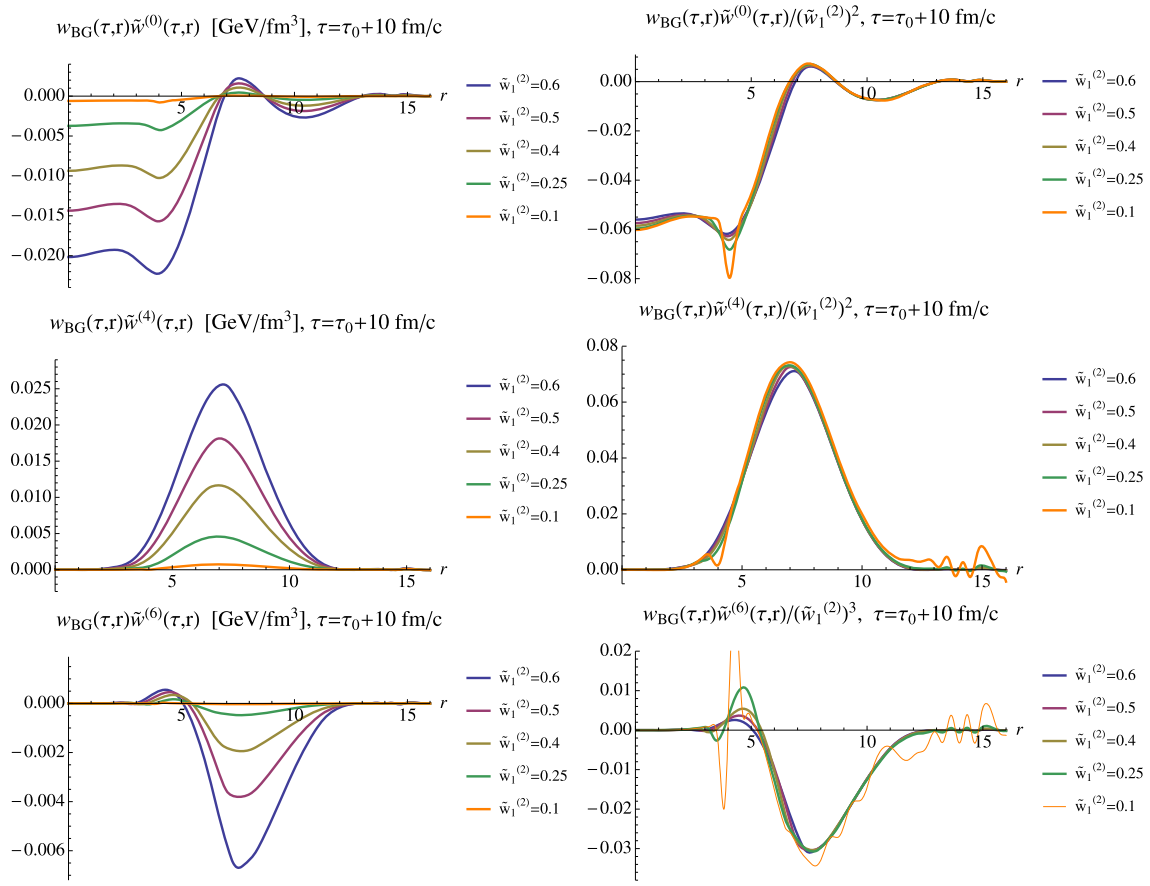

Fig. 2. Left column: The zeroth, fourth and sixth harmonic perturbations induced by an initial fluctuation in the second harmonic, shown for different values of the initial weight $\tilde{w}_1^{(2)}$. Right column: The same results but rescaled by the second (third) power of the weight $\tilde{w}_1^{(2)}$. This scaling establishes that $\tilde{w}^{(0)}(\tau,r)$ and $\tilde{w}^{(4)}(\tau,r)$ ($\tilde{w}^{(6)}(\tau,r)$) can be understood as overtones that are induced by the initial second harmonic perturbation as a perturbative second (third) order correction to (2). The short-range fluctuations in the rescaled $\tilde{w}^{(6)}(\tau,r)$ result from amplifying the numerical uncertainties of very small number by a large scaling factor $(1/\tilde{w}_1^{(2)})^3=1000$.

our formalism) [5,10–12,21] and that a combination of linear plus quadratic terms in eccentricities is a good "predictor" for the hydrodynamic response in a large set of realistic collisions, in the sense that an appropriately defined Pearson coefficient is close to unity [12].

We further note that the perturbative series (8) contains also information about the azimuthal orientation of non-linear corrections. This is in particular relevant for reaction plane correlations such as the ones studied in Refs. [7,21–23]. The findings recalled here were demonstrated mainly on the level of particle spectra after the fluid has frozen out. There are only few comments that attribute specific non-linear corrections either to the hydrodynamic evolution [5] or to the hadronic freeze-out [24].

We now turn to a quantitative test of the perturbative series (7). According to this equation, fluctuations initialized as in Fig. 1 with a *single* mode of weight $\tilde{w}_l^{(m)}$ receive corrections to second order in $\tilde{h}_i(\tau_0)$ that do not appear in the time-evolved harmonics $\tilde{h}_i^{(m)}$, but in the harmonics $\tilde{h}_i^{(2m)}$ and $\tilde{h}_i^{(0)}$. Also the third order correction enters the fluctuating fields in $\tilde{h}_i^{(3m)}$ (and it enters in $\tilde{h}_i^{(m)}$ as a correction that is subleading by two orders compared to the leading linear response). Fig. 2, shows that the non-linearities observed in the overtones $\tilde{h}_i^{(2m)}$, $\tilde{h}_i^{(0)}$ ($\tilde{h}_i^{(3m)}$), scale indeed to high accuracy with the second (third) power of $|\tilde{w}_1^{(2)}|$, as expected from (7). Also, the last row of Fig. 1 illustrates that the sizeable non-linearities in $\tilde{h}_i^{(m)}$ observed for extreme values of $\tilde{w}_l^{(m)}$ scale as expected from (7). This suggests that for the entire physically relevant range of values $|\tilde{w}_l^{(m)}|$, the perturbative series (2) provides an ordering principle that explains how linear and non-linear contributions feed into different azimuthal modes m, and how they scale characteristically different with the initial amplitudes $\tilde{w}_l^{(m)}$.

Eq. (2) explains also the structure and symmetries of the hydrodynamic interactions between initial perturbations with different wave numbers. Fig. 3 illustrates this point with a case for which two perturbations $\tilde{w}_2^{(2)}$, $\tilde{w}_1^{(3)}$ are embedded on top of the initial background fields. We have checked that the second (third) harmonics $\tilde{w}^{(2)}(\tau,r)$ ($\tilde{w}^{(3)}(\tau,r)$) of the fluid dynamic response scale almost linearly with the initial weight $\tilde{w}_2^{(2)}$ ($\tilde{w}_1^{(3)}$) and that they agree to high accuracy with the response to an initial configuration in which only one mode $\tilde{w}_2^{(2)}$ ($\tilde{w}_1^{(3)}$) is embedded on top of w_{BG} (data not shown). Also, $\tilde{w}^{(4)}(\tau,r)$ scales with the square of $\tilde{w}_2^{(2)}$ (data not shown), similarly to the case shown in Fig. 2. For studying interactions between different modes, we show in Fig. 3 the first and fifth harmonics that according to Eq. (8) are the only harmonics that receive leading second order contributions proportional to $\tilde{w}_2^{(2)}\tilde{w}_1^{(3)}$. If $\psi^{(2)}\neq\psi^{(3)}$, then the responses $w_{BG}\tilde{w}^{(1)}$ and $w_{BG}\tilde{w}^{(5)}$ have both a real and an imaginary part. Both parts exhibit the expected scaling with $\tilde{w}_2^{(2)}\tilde{w}_1^{(3)}$, as seen in Fig. 3. Also, according to (8), the phases of the first and fifth harmonics are determined by the orientations of the initial perturbations. The comparison with the full numerical results in the middle panel of Fig. 3 shows that this perturbative expectation is realized approximately (strong deviations are seen only for values of the radius r

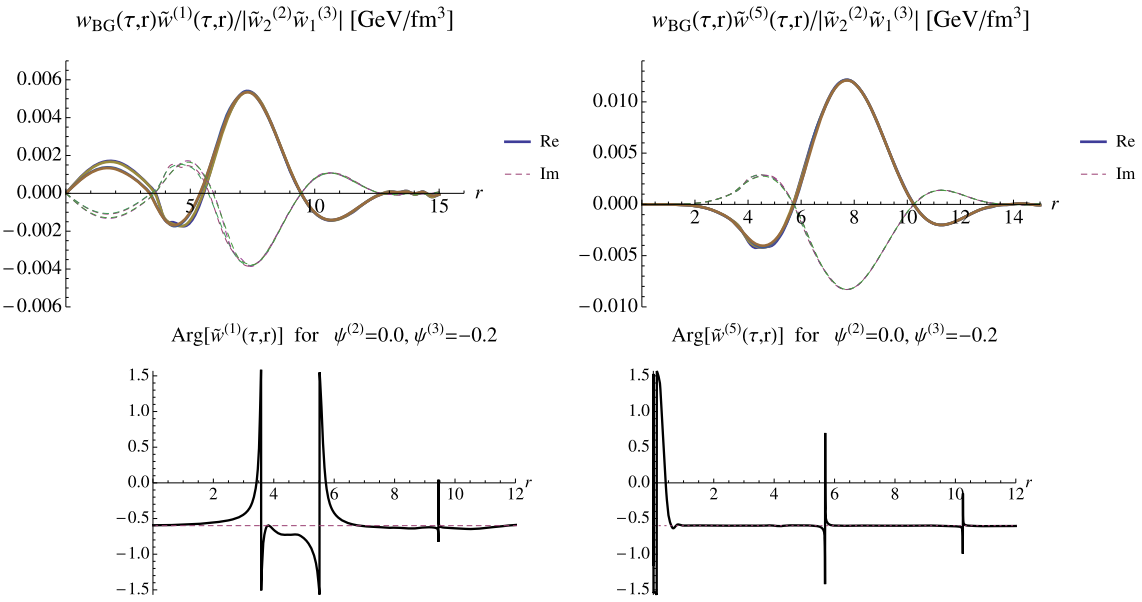

Fig. 3. Results from ECHO-QGP for evolving up to $\tau = \tau_0 + 10$ fm/c on top of the background of Fig. 1 an initial condition composed of two basis modes with weights $\tilde{w}_2^{(2)}$, $\tilde{w}_1^{(3)}$ and angles $\psi^{(2)} = 0$ and $\psi^{(3)} = -0.2$. Upper row: Real and imaginary parts of the first ($w_{BG}\tilde{w}^{(1)}$) and fifth ($w_{BG}\tilde{w}^{(5)}$) harmonics of the enthalpy. The curves shown are for the four combinations of $\tilde{w}_2^{(2)} = 0.1, 0.25$ and $\tilde{w}_1^{(3)} = 0.1, 0.25$ and illustrate scaling behavior. Middle row: The phase Arg[$\tilde{w}^{(m)}(\tau, r)$] of the m-th harmonic mode (solid) compared to the perturbative expectation (dashed line) based on Eq. (8).

for which Re[$\tilde{w}^{(m)}$] and Im[$\tilde{w}^{(m)}$] approach zero and for which the orientation is thus not well defined). We have checked that Eq. (8) accounts also quantitatively for the more complicated dependence of higher harmonics that receive non-linear corrections from more than one term in (7). Here, this is the case e.g. for $w_{BG}\tilde{w}^{(6)}$ that receives corrections of second order in $\tilde{w}_1^{(3)}$ and of third order in $\tilde{w}_2^{(2)}$.

Realistic initial conditions for the fluid dynamic evolution of heavy ion collisions are expected to involve fluctuations on many different length scales and with large amplitude. Could it be that the perturbative series (2) provides for the case of simple initial conditions with few fluctuating modes an understanding for how linear response and non-linearities arise, but that it is inadequate for dealing with the complexity of a realistic heavy ion collision? To lay such concerns at rest, we have embedded single basis modes in realistic initial conditions with many and large fluctuations. Fig. 4 shows such an initial distribution. It is constructed by subtracting from an arbitrary initial condition generated by a Glauber model the contribution leading to a second harmonic and adding then the perturbation of (5). In this way, we have an analytically controlled initial perturbation on top of a realistically fluctuating background, and we can extract this initial perturbation and the time dependence of its fluid dynamic response via Fourier analysis. The lower panel of Fig. 4 shows that this dynamical response in an event with realistic fluctuations is described to high accuracy by the response established in Fig. 1.

In summary, the evolution of initial anisotropic density perturbations as determined numerically with the fluid dynamics solver ECHO-QGP seems to follow a simple pattern that can be understood order-by-order in a perturbative expansion for small deviations from an azimuthally symmetric event-averaged background. The leading order is linear and modes with different azimuthal wave numbers do not mix. Quadratic and higher orders can be seen as next-to-leading order corrections. They influence modes with azimuthal wave numbers that can be written as sums (or differences) of the seed wave numbers. If non-linear couplings are numerically small, the higher harmonics generated by two-mode or three-mode interactions will often be small in comparison to initially present and linearly evolving perturbations. But also for initial conditions for which non-linear contributions may be sizable, we have shown that the perturbative series expressed by Eqs. (2) or (7) provides a useful ordering scheme for understanding the dependence of non-linearities on the amplitudes of initial fluctuations. This motivates a more formal and thorough development of this kind of perturbation theory. In this context, it would be also interesting to consider initial fluctuations in vorticity where one may expect on general physics grounds that non-linearities play a more important role [25]. We also note that the relative importance of linear and non-linear terms may depend on the dissipative properties of the medium [11,15]. We intend to study the dependence on η/s in subsequent work.

While our studies clearly demonstrate that the hydrodynamic response to initial fluctuations is predominantly linear for a wide range of physically relevant amplitudes $|\tilde{w}_l^{(m)}| < 0.5$, we caution that this does not imply that experimental observables must be dominated by linear contributions. Consider for instance an experimentally observable quantity in the fifth harmonic, such as v_5. Based on (2) and Fig. 3, we expect that it receives linear contributions $\propto |\tilde{w}_l^{(5)}|$ and quadratic contributions $\propto |\tilde{w}_l^{(2)}\tilde{w}_{l'}^{(3)}|$. Even if the hydrodynamic response to any of the modes $m = 2$, $m = 3$ and $m = 5$ is predominantly linear, the initial conditions for an event sample may be such that $|\tilde{w}_l^{(5)}|$ is small against $|\tilde{w}_l^{(2)}\tilde{w}_{l'}^{(3)}|$ – in this case, v_5 would be dominated by the non-linear contribution of the hydrodynamic response, but the dependence of this dominant non-linear response on the initial weights $|\tilde{w}_l^{(m)}|$ would be described by the perturbative series (2). Thus, our finding that the hydrodynamic response can be based on a perturbative series with a leading linear response term does not disagree with the result of simulations [5] that show that observables can be dominated by non-linearities in the hydrodynamic response. Rather, the perturbative series (2) shows how such non-linearities arise dynamically and we intend to exploit this further in subsequent work.

We note that non-linear corrections to linear response can come both from the hydrodynamic evolution studied here and

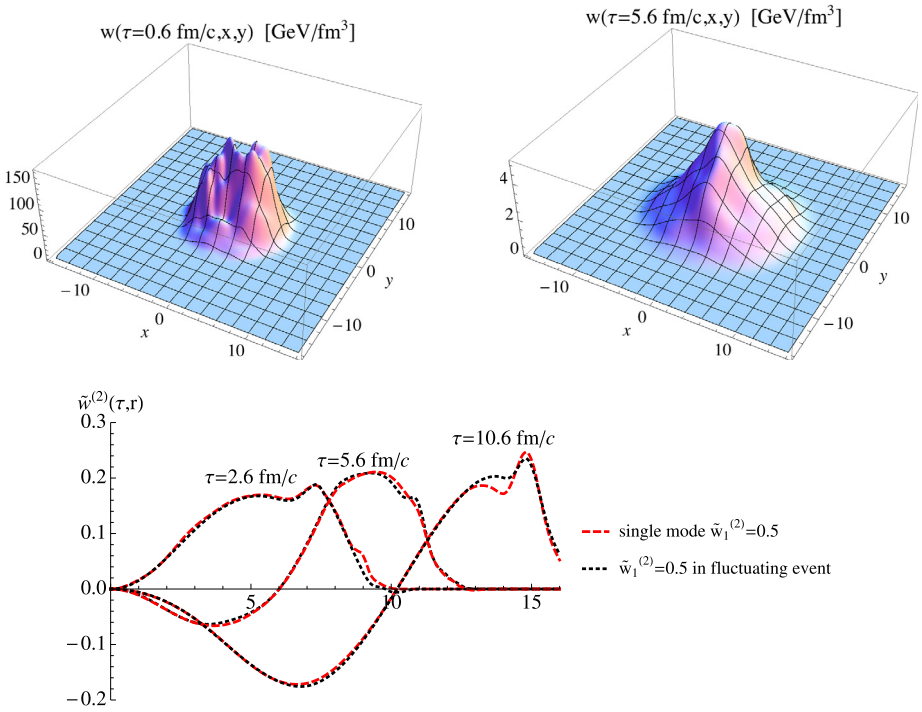

Fig. 4. Upper panels: Left: Example of an initial condition with many fluctuating modes $\tilde{w}_l^{(m)}$, $m \neq 2$, and the mode $\tilde{w}_1^{(2)} = 0.5$ on top of the background w_{BG}. Right: The same distribution, evolved up to $\tau = \tau_0 + 5$ fm/c. Lower panel: The second harmonics $\tilde{w}^{(2)}(\tau, r)$ extracted for different times τ. Results extracted from the fluctuating event shown in the upper panel are compared to the case shown in Fig. 1 in which $\tilde{w}_1^{(2)} = 0.5$ is the only mode embedded on top of a smooth background. This illustrates that the assumption of a predominantly linear response on top of a suitably chosen background is applicable for realistic initial conditions that display strong fluctuations.

from non-linearities in the hadronization process. There are some first observations that disentangle between both mechanisms [5,24], but given the significantly different physics tested in both stages, more detailed studies would be desirable. In particular, the present work could be extended to a characterization of non-linearities in the freeze-out process.

Acknowledgements

AB is supported by European Research Council grant HotLHC ERC-2011-StG-279579. ECHO-QGP was developed within the Italian PRIN 2009 MIUR project “Il Quark-Gluon Plasma e le collisioni nucleari di alta energia”, grant No. 2009WA4R8W. We also thank F. Becattini for helping to make this collaboration possible.

References

[1] U.W. Heinz, R. Snellings, arXiv:1301.2826 [nucl-th].
[2] C. Gale, S. Jeon, B. Schenke, Int. J. Mod. Phys. A 28 (2013) 1340011.
[3] B. Hippolyte, D.H. Rischke, Nucl. Phys. A 904–905 (2013) 318c, arXiv:1211.6714 [nucl-ex].
[4] D.A. Teaney, Review for ‘Quark Gluon Plasma 4’. R.C. Hwa, X.N. Wang (Eds.), World Scientific, Singapore, arXiv:0905.2433 [nucl-th].
[5] Z. Qiu, U.W. Heinz, Phys. Rev. C 84 (2011) 024911.
[6] B. Schenke, S. Jeon, C. Gale, Phys. Rev. C 85 (2012) 024901.
[7] R.S. Bhalerao, M. Luzum, J.-Y. Ollitrault, Phys. Rev. C 84 (2011) 034910.
[8] B. Schenke, P. Tribedy, R. Venugopalan, Phys. Rev. Lett. 108 (2012) 252301.
[9] H. Holopainen, H. Niemi, K.J. Eskola, Phys. Rev. C 83 (2011) 034901.
[10] D. Teaney, L. Yan, Phys. Rev. C 83 (2011) 064904.
[11] D. Teaney, L. Yan, Phys. Rev. C 86 (2012) 044908.
[12] F.G. Gardim, F. Grassi, M. Luzum, J.-Y. Ollitrault, Phys. Rev. C 85 (2012) 024908.
[13] H. Petersen, R. La Placa, S.A. Bass, J. Phys. G 39 (2012) 055102.
[14] W.-L. Qian, P. Mota, R. Andrade, F. Gardim, F. Grassi, Y. Hama, T. Kodama, arXiv:1305.4673 [hep-ph].
[15] H. Niemi, G.S. Denicol, H. Holopainen, P. Huovinen, Phys. Rev. C 87 (2013) 054901, arXiv:1212.1008 [nucl-th].
[16] W.-T. Deng, Z. Xu, C. Greiner, Phys. Lett. B 711 (2012) 301.
[17] S. Floerchinger, U.A. Wiedemann, Phys. Lett. B 728 (2014) 407, arXiv:1307.3453.
[18] S. Floerchinger, U.A. Wiedemann, Phys. Rev. C 88 (2013) 044906, arXiv:1307.7611 [hep-ph].
[19] L. Del Zanna, V. Chandra, G. Inghirami, V. Rolando, A. Beraudo, A. De Pace, G. Pagliara, A. Drago, et al., Eur. Phys. J. C 73 (2013) 2524, arXiv:1305.7052 [nucl-th].
[20] Z. Qiu, C. Shen, U. Heinz, Phys. Lett. B 707 (2012) 151.
[21] D. Teaney, L. Yan, arXiv:1312.3689 [nucl-th].
[22] G.-Y. Qin, B. Muller, Phys. Rev. C 85 (2012) 061901, arXiv:1109.5961 [hep-ph].
[23] J. Jia, D. Teaney, Eur. Phys. J. C 73 (2013) 2558, arXiv:1205.3585 [nucl-ex].
[24] N. Borghini, J.-Y. Ollitrault, Phys. Lett. B 642 (2006) 227, arXiv:nucl-th/0506045.
[25] S. Floerchinger, U.A. Wiedemann, J. High Energy Phys. 1111 (2011) 100, arXiv:1108.5535 [nucl-th].